Düzce University
Journal of Science & Technology

Research Article

Determination of Structural Parameters and Design of Experiments Approach-Based Optimisation of Steel Track Undercarriage Link

Kübra POLAT [a,*], Mehmet Murat TOPAÇ [a], Onur ÇOLAK [a], Ali Özgür GÜNAY [b]

[a] *Department of Mechanical Engineering, Faculty of Engineering, Dokuz Eylül University, İzmir, TÜRKİYE*
[b] *Smart İş Makinaları San. Tic. A.Ş., Manisa, TÜRKİYE*
** Corresponding author's e-mail address: k.polat@ogr.deu.edu.tr*
DOI: 10.29130/dubited.1472942

ABSTRACT

In this study, the design and optimisation processes of the link to be used in the steel track undercarriage system of a tracked vehicle are summarised. In the first stage, a preliminary model was created by considering existing design examples and constraints. Two different Finite Element (FE) models were built using the maximum driving torque and track - ground contact forces. According to the results obtain from the analyses, three critical regions where stress concentration occurs, were identified. Seven structural design parameters were chosen to minimise stress concentrations in these regions. A Design of Experiments-based optimisation study was performed using these parameters. After obtaining new dimensional values, a new link design was created. The FE analyses conducted for maximum torque case showed that approximately decrease of 61%, 55%, and 20% was obtained in terms of stress concentration at the first, second, and third critical regions, respectively. Under the effect of vertical and lateral forces, the improvement percentages are 63%, 26%, and 31%, in the same order. It was observed that the stress values obtained at the critical regions of the new design under the failure loads, were below the permissible values.

Keywords: *Design of Experiment (DoE), Steel track undercarriage, Tracked Vehicles*

Çelik Paletli Yürüyüş Sistemi Baklasının Yapısal Parametrelerinin Belirlenmesi ve Deney Tasarımı Yaklaşımıyla Optimizasyonu

ÖZ

Bu çalışma kapsamında, bir paletli taşıtın çelik paletli yürüyüş sisteminde kullanılan baklanın tasarım ve optimizasyon süreçleri özetlenmiştir. İlk aşamada, uygulanmış tasarım örnekleri ve tasarım kısıtları dikkate alınarak bir ön model oluşturulmuştur. Baklaya etkimesi beklenen maksimum tahrik torku ve
temas kuvvetleri yardımıyla iki farklı Sonlu Elemanlar (SE) modeli kurulmuştur. Bu model yardımıyla parça üzerinde gerilme açısından üç kritik bölge belirlenmiştir. Gerilme yığılmalarının azaltılması için bakla üzerinde yedi adet yapısal tasarım parametresi seçilmiştir. Bu parametreler kullanılarak gerçekleştirilen Deney Tasarımı tabanlı bir optimizasyon çalışması sonucunda elde edilen boyutsal değerler yardımıyla, yeni bakla tasarımı oluşturulmuştur. Motordan sisteme maksimum tork uygulanması durumu için yapılan SE analizleri, birinci, ikinci ve üçüncü kritik bölgelerde gerilme yığılması açısından sırasıyla, yaklaşık %61, %55 ve %20 oranlarında iyileşme elde edildiğini göstermiştir. Düşey ve yanal kuvvet etkisi altında ise iyileşme yüzdeleri, aynı sıralamayla, %63, %26 ve %31'dir. Sonuç olarak, elde edilen parametrelerle gerçekleştirilen yeni bakla tasarımında, kritik bölgelerde elde edilen gerilme değerlerinin, hasar oluşumuna neden olan değerlerin altında kaldığı görülmüştür.

Anahtar Kelimeler: *Deney Tasarımı (DT), Paletli yürüyüş sistemi, Paletli Taşıtlar*

Received: 24/04/2024, Revised: 21/08/2024, Accepted: 09/09/20242024

I. INTRODUCTION

Tracked walking systems have a wide range of applications in many different disciplines such as defence, construction, mining, agriculture and mobile robotics. These vehicles were initially designed as a "portable railway" which are laid in front of the road wheels and mounted on the vehicle during the motion [1]. With the advancement of technology, these vehicles have become more durable and manoeuvrable. Tracked vehicles are advantageous compared to wheeled vehicles especially in off-road conditions such as soil, mud and snow. The main reasons for this advantage are the larger contact area and longer tyre contact length of tracked vehicles compared to wheeled vehicles [1,2]. At the same time, the larger total contact area of tracked vehicles allows them to contact a larger amount of the ground surface. This is one of the main reasons why the traction of tracked vehicles is higher than that of wheeled vehicles. Because it is known from the literature that increasing the tyre contact length and area increases the traction of a wheeled vehicle on the terrain [1]. Figure 1 shows the crawler excavator used in this study.

Figure 1. *General view of the steel track undercarriage system (Courtesy of Smart İş Makinaları San. Tic. A.Ş.).*

Failures can occur on the undercarriage system of tracked vehicles under overload and harsh operating conditions. This can result from various reasons such as design and/or manufacturing defects, inconvenient working conditions and environmental factors. In open literature, failure investigation studies have been reported for these systems [3-8]. Zhi-wei et al. [4], investigated the failure of two crawler links of a tracked vehicle used for dredging. Characterisation studies show that, undesired residues in the track link material caused the component to become brittle. In the study by Bošnjak et al. [5], the chain link failure was investigated by metallographic examination and the Finite Element Method (FEM) for a specified lifetime of a tracked vehicle. As a result of the analysis and tests, it was found that the mechanical properties of the material significantly deviated from the specifications. In addition, the micro and macro cracks were detected in the material structure and it was shown that the failure was caused by manufacturing defects. In another study by Bošnjak et al [6], various methods were used to determine the cause of failure of track links. As a result of the analyses, it was determined that the increase in sulphur content in the link material caused the failure. Zhao et al [7] investigated the stresses on the link under different steering conditions of the excavator at low speeds. In the FE analyses, it was observed that the maximum stress value in the chain links was lower than the yield strength, but there was a crack in the corner where the bolt holes of the chain link on the lateral force bearing side were located. Literature studies show that the failures in the track links are generally caused by manufacturing defects and fatigue.

Tracked excavators consist of parts such as track (1), track shoe (2), link (3), bushing connection pin (4), idler (5), sprocket (6) and track tensioning system shown in Figure 2. The links are connected by pins and bushes to hold the chain together. The drive wheel transfers the drive torque from the engine to the track chain via the links and thus enables the chassis (7) to move on the ground. The track rollers (8), which are rotatable mounted on the chassis, roll on the links. The chassis' vertical load is transmitted

via the rollers to the links and the track shoes connected to them. In this way, a uniform pressure distribution is provided on the ground contact surface and the movement. This enables the vehicle to have better traction characteristics in difficult ground conditions [9,10]. The failure of the track undercarriage system during operation in various surface conditions causes material and temporal losses [4,7].

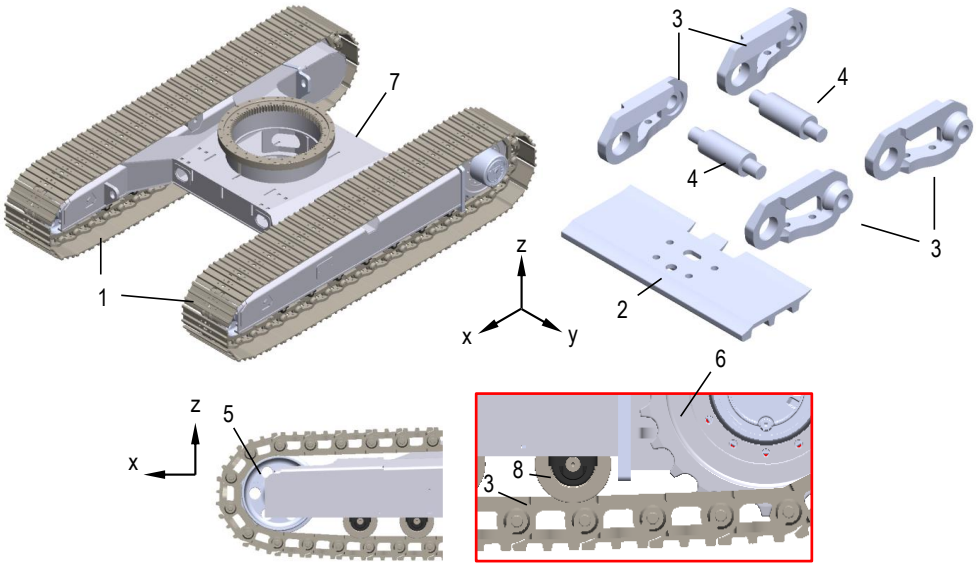

Figure 2. *General view of the steel crawler system used in an excavator and layout of structural elements [9]*

In this study, the design and optimisation processes of the link to be used in the steel track system of a tracked vehicle shown in Figure 3 are summarised. In the first step, a preliminary model was constructed by considering the applicable design examples and constraints. Two different Finite Element (FE) models were also built with the help of the maximum drive torque and link contact forces. These models used to identify three critical regions on the part in terms of stress concentrations. Seven structural design parameters were selected to minimise stress concentrations in these regions. Using these parameters, a new link design was generated using the dimensional values obtained from a Design of Experiments-based optimisation study. It was observed that the new design obtained as an optimization result did not exceed the fatigue stress value obtained from the literature [7].

As mentioned, there are studies in the open literature based on investigating the cause of link failure; however, to the best of the authors' knowledge, studies which summarise a complete design process of a steel crawler excavator link using DoE-based optimisation is not available in the open literature.

II. MATERIAL AND METHOD

A. LOAD MODEL AND FINITE ELEMENT MODEL

The solid models were imported into ANSYS® Workbench 2020R2 commercial FE software for stress analysis. The load scenario in which the chassis operates at low speed where the right and left tracks moving in opposite directions relative to each other, i.e. a pivot steering around the vertical axis, was selected as the load scenario.

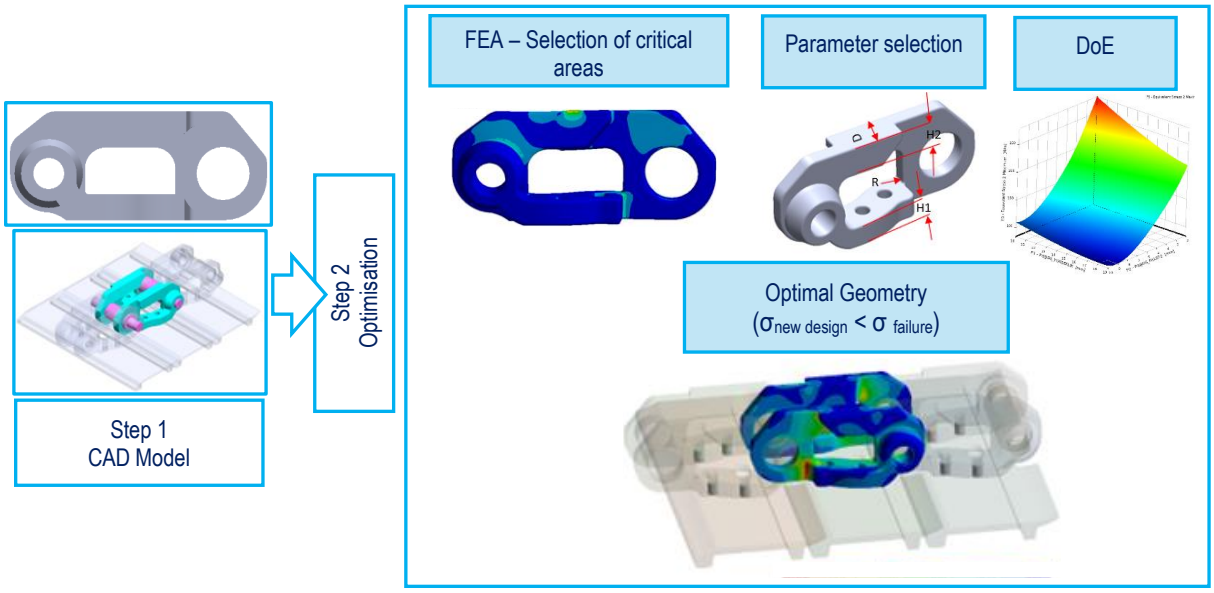

Figure 3. *Study Summary*

According to this load model, two different FE models including the maximum drive torque and contact forces were built. For low speeds the load was assumed to be uniformly distributed. The idealised loads acting on the crawler are as shown in Figure 4 [11,12].

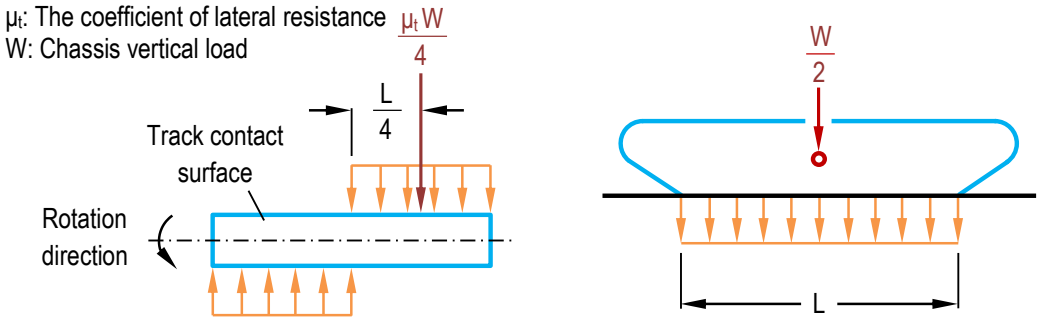

Figure 4. *Lateral resistance acting on the track during low-speed rotation (according to [12])*

For the maximum drive torque model, the maximum tensile force was calculated via maximum engine torque and the drive sprocket diameter provided by the manufacturer. For the second load model, the vertical and lateral forces between the roller and link utilised for the fatigue analysis of a track chain link used in a similar weight excavator were obtained from the literature [7]. The two different loading models summarised in Figure 5. In the first case, named as case "a", the link begins to wrap on the drive wheel sprocket and operates under maximum tensile force. In the second case (or case "b"), the link is in contact with both the ground and the roller.

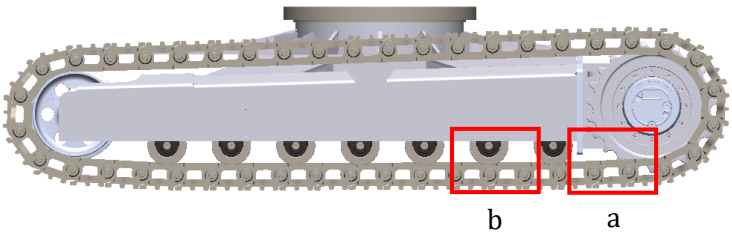

Figure 5. (a) *Maximum traction case and* ***(b)*** *both in contact with the ground and contact force by the roller*

These two selected load models were applied to both the single link model and the sub-model. By this way, the stress distributions for both models were obtained. In the first model, the tensile force acting on the single link was applied as half of the total tensile force (F_x) through pin A in the -x axis direction. Here, load distribution was assumed symmetric as shown in Figure 6.a. The translational movement of the pin A in the force direction was allowed, while the translational and rotational movements in other directions were constrained. In the latter model, the rotational movement around the drive sprocket and the horizontal movement of the link are unconstrained. Here, pin D is fixed. In order to model the contact forces that occur when the rollers pass over the link, the contact points of the rollers on the link were determined first. These regions were separated on the part. Then, vertical and lateral forces were applied to the separated contact area in addition to the tensile force. Due to the distance between the centres of the two rollers mounted on the chassis, during the movement of the track, only a single roller can be in contact with a link at any given time, during the interval when the roller contacts and then leaves the link. In the sub-model shown in Figure 6.c, the tensile force Fx acting on the link is applied through pin A in the -x axis direction. The rotational freedom of pin D is constrained and the friction between links, rollers and pins is not considered in the model. Due to the surface contact resistance acting on the track shoe, the idealised longitudinal and lateral forces (R and S), which are assumed to act on the chassis from the road, are modelled as uniformly distributed surface pressure on the track shoe.

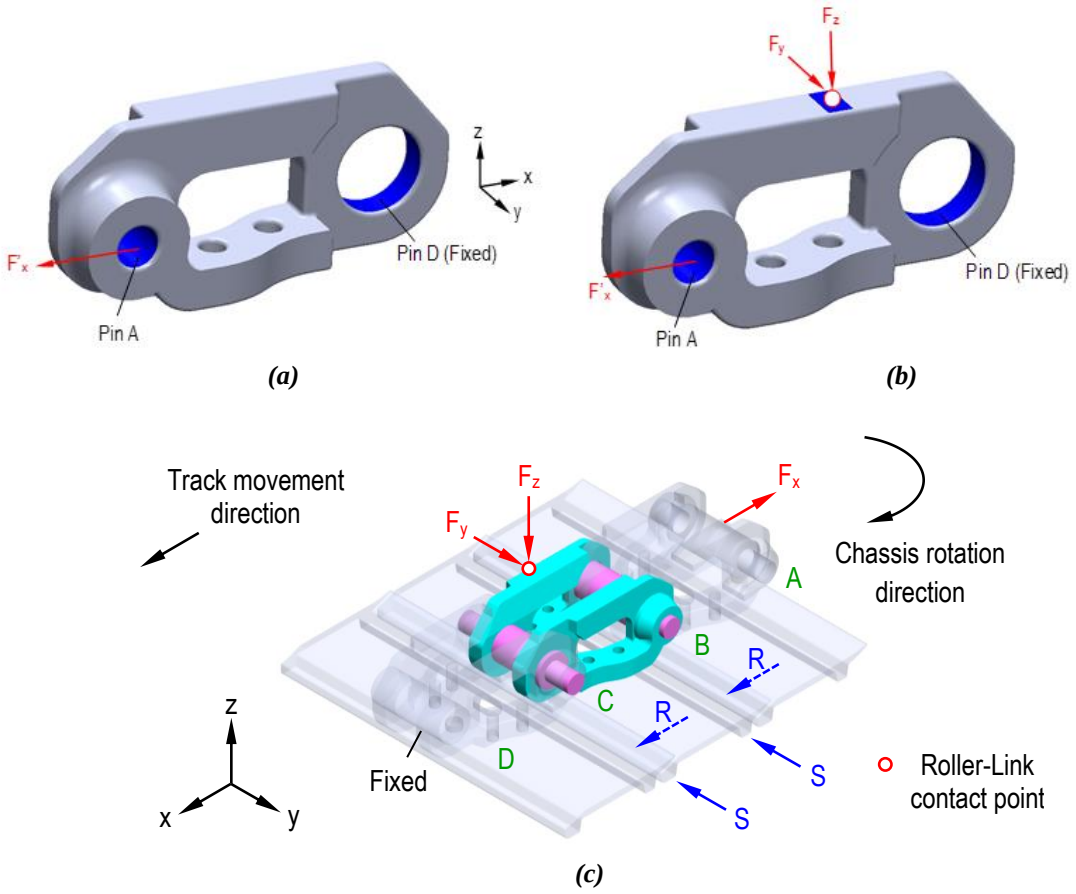

Figure 6. (a) *Maximum tension model,* ***(b)*** *Model subjected to crushing by rollers and* ***(c)*** *Sub-model [9]*

B. DESIGN OF EXPERIMENTS -RESPONSE SURFACE METHOD

Design of Experiments (DoE) and Response Surface Methodology (RSM) are methods often used in engineering to optimise the performance of a system or process. These methods are used together to study the relationship between input parameters, known as design variables, and the response of the system, known as output parameters. This method helps to determine the effects of variables on the system and their optimal levels. In other words, in order to systematically investigate the effect of

multiple variables in the system on the response, DoE is generally used. To build a model describing the relationship between the design variables and the system response, response surface experiments with specific rules are required. The results obtained from these experiments allow us to determine the effects of the design variables on the system response and using this information we can build a mathematical model. The regression model for a second order RS can be defined as follows [13];

$$y = \beta_0 + \sum_{i=1}^{k} \beta_i x_i + \sum_{i \leq j}^{k} \beta_{ij} x_i x_j + \varepsilon \quad (1)$$

if written in matrix form:

$$y = X\beta + \varepsilon \quad (2)$$

where, y is the observation vector, X is the model matrix, β is the vector containing partial regression constants and ε is the error vector [13]. In this study, a table was created by the software using the DoE method for the allowable values of the input parameters using design examples. The optimisation was performed using ANSYS Workbench® software. Central Composite Design (CCD) was used to determine the optimum parameter values. CCD is an option available in the DoE module design table and a detailed description of this procedure is available in the literature [14-16].

III. RESULTS AND DISCUSSION

C. DESIGN CONSTRAINTS AND PRELIMINARY DESIGN

In the first stage, a preliminary solid model was designed considering the existing design examples [17,18] and constraints. The link geometries were firstly designed in two groups: In the first group pin slot structure was altered where upper and lower height values remain constant. In the second group, both height values were changed additionally. While constructing these models, the penetration of the parts in the range of the link rotation angle when it is wrapped on the drive wheel and the distances between the drive wheel and the links were taken into account, as shown in Figure 7. Then, a preliminary model was selected among these two groups. Figure 8 shows the FEA results of the link geometries.

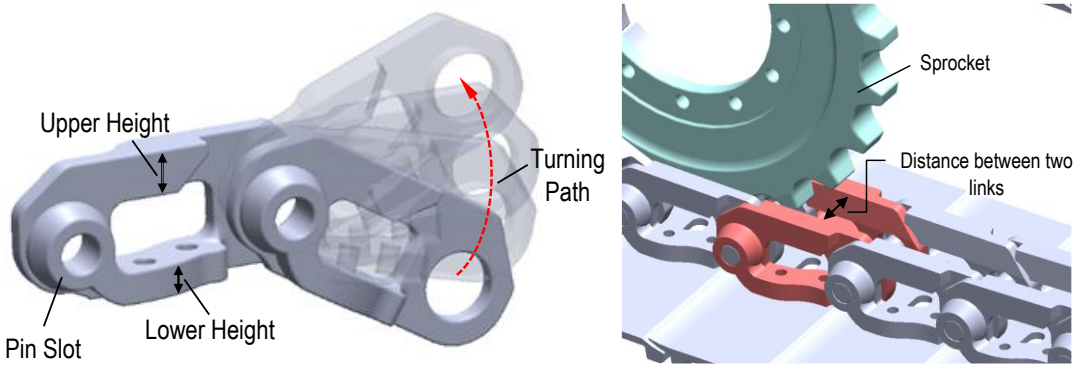

Figure 7. *Working envelope of the chain link*

ANSYS® Workbench 2020R2 commercial FE software was used for the stress analysis of the link. SOLID187 element type consisting of a total of ten nodes, each with three linear degrees of freedom, was used in the FE model. The analysis model consists of 256,810 elements and 368,334 nodes.

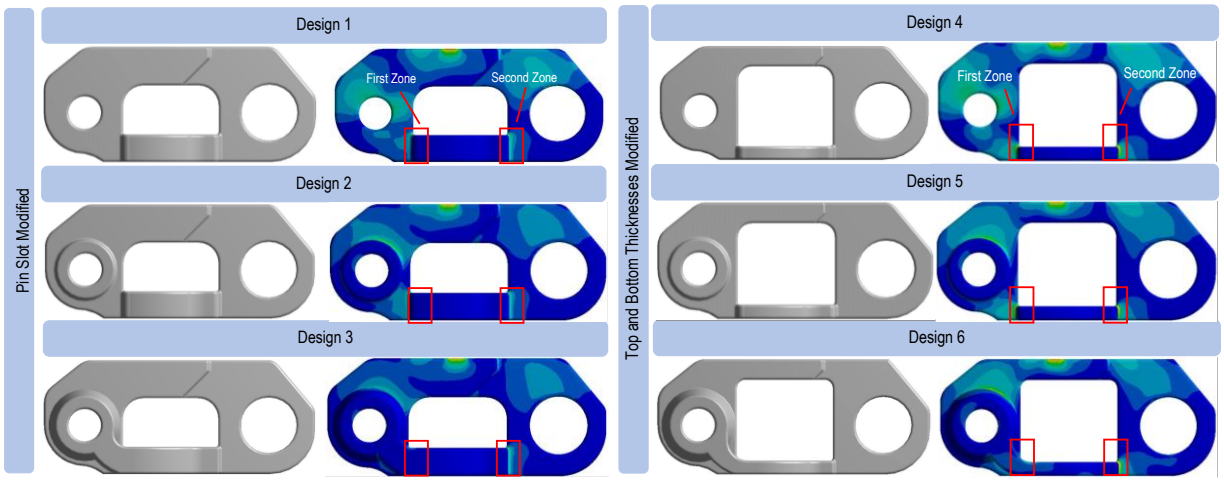

Figure 8. *Link designs with different geometries created for preliminary model selection*

According to the FEA results, the stress concentration values at the first and second regions of Design 4, 5 and 6 approximately twice compared to Designs 1, 2 and 3. Therefore, the preliminary model was selected from the group in which the pin slot was replaced. The maximum stress values of Design 1 and Design 2 is three times greater than Design 3 in the first region, while this value increases up to five times in the second region. For this reason, Design 3 was chosen as the most suitable preliminary design for both regions. Hence, critical regions were identified through this model. Figure 9 shows a comparison of the stress concentrations for both regions of whole designs. Here, the stress values of the preliminary model shown as PM assumed as a reference. Other stress values normalised to these values.

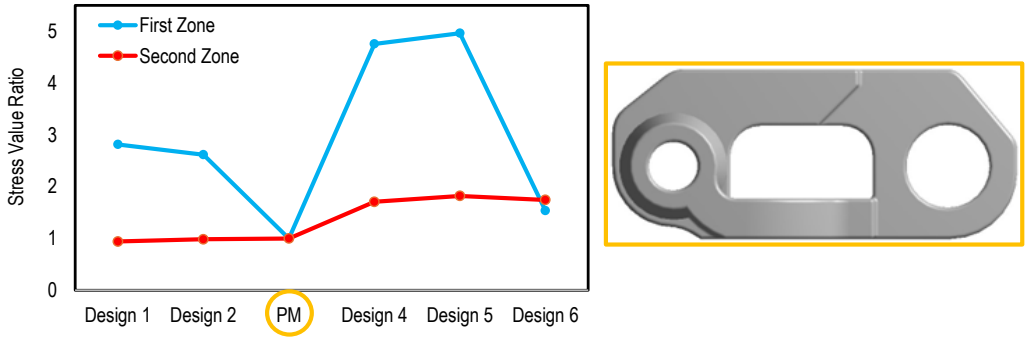

Figure 9. *Comparison of first and second zone stresses of links with different geometries according to the selected preliminary model*

D. PARAMETRIC OPTIMISATION

According to the FEA results of the preliminary model, three critical stress regions were identified for the DoE. In the selection of these regions, the principal stress distribution on the link was analysed and it was found that the selected regions operate mainly under tensile stress. The area selected as the first critical region is a zone where failure has been observed [7]. The second and third critical regions were selected for the optimisation study as the stress concentration occurring in these regions is higher than the stress value at which failure occurs [7]. Figure 10 shows the stress distributions in the critical regions determined on the link.

To minimise stress concentrations in these critical regions, seven structural design parameters were selected. Then, a DoE based optimisation study was performed using these parameters and a new link design was built using the obtained values. Figure 11 show the critical regions and selected design parameters.

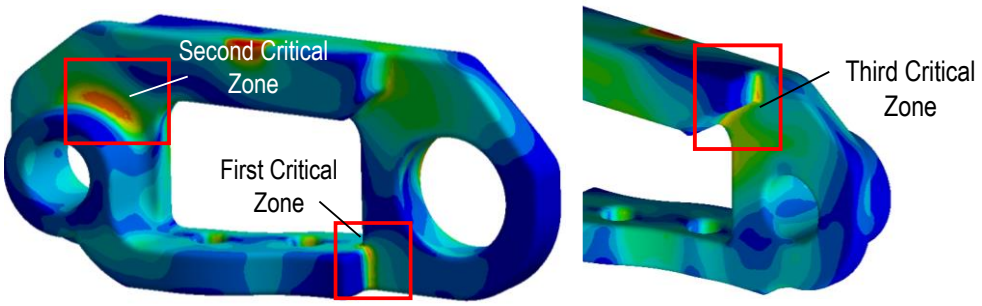

Figure 10. *Selected critical areas on the link*

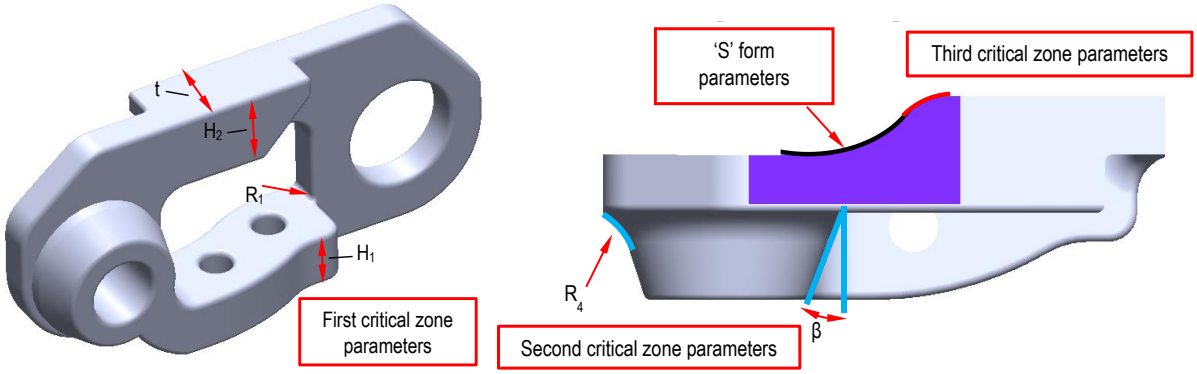

Figure 11. *Parameters of the link*

Firstly, the effect of design parameters such as fillet radius (R_1), part thickness (t), lower part height (H_1) and upper part height (H_2) on the stress concentration at the first critical region was analysed and the optimum design values were determined. The RS graphs were generated by using the maximum stress (σ_{max}) values calculated for the design points. The parameter's variation ranges determined by considering Figure 7. To reduce the stress concentration at the first critical region, design improvements were also done. The RS graphs obtained according to the maximum stress as a result of DoE are shown in Figure 12.

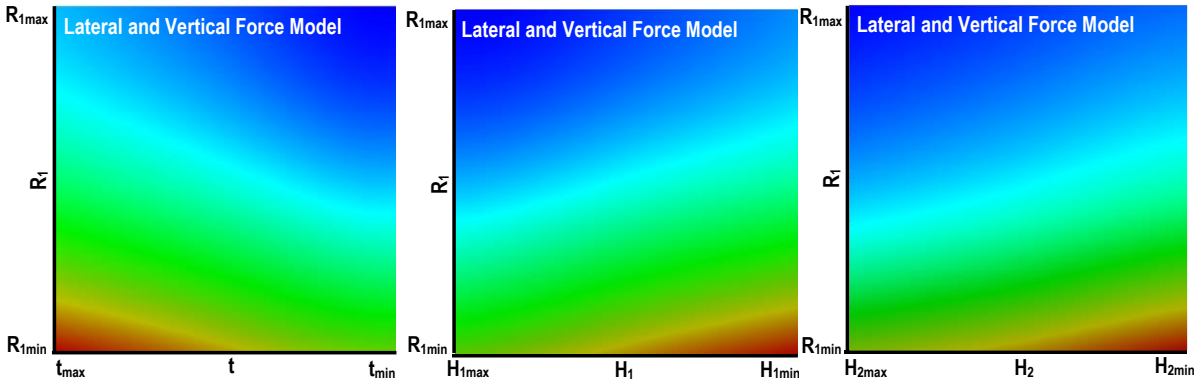

Figure 12. *Response Surface plots obtained according to the maximum stress at the first critical zone*

In the first critical region, the effect of the fillet radius (R_1), which is approximately determined as 62 %, is higher than the other parameter effects. In the maximum torque model, its effect is greater than the lateral and vertical force model. At the first critical region, the effect of the upper height was found to be approximately 12% for the maximum torque model. In the other load model, this value is 15%. Figure 13 shows the effect percentages of the parameters.

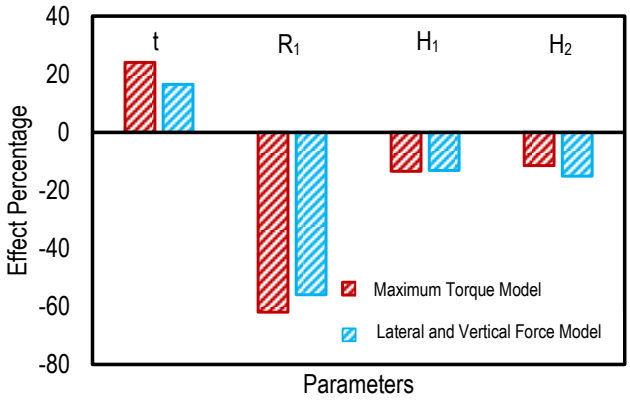

Figure 13. *Effect percentages of parameters in the first critical region*

In the DoE study of the third critical region, the structure of the upper part was given an 'S' form to ensure a smooth transition. Two radii were defined as shown in Figure 14.a. The R_2 parameter was found to have the highest effect on stress concentration. When the model for specific R_2 and R_3 values was analysed for two different load cases, a 57% increase in stress concentrations was observed in the second load model compared to the first model. This result shows that, a specific load model may not be sufficient for parameter selection. The effect of these parameters on the stress values over the third critical region is shown in Figure 14.b.

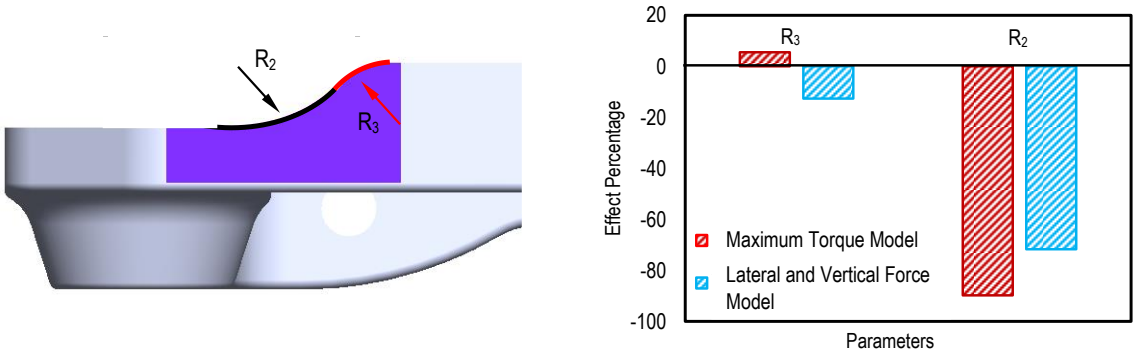

Figure 14. *Effect percentages of parameters in the third critical region*

After determining the optimal values of the first and third critical region parameters, the second DoE study was carried out for the pin slot region (second critical region) optimisation. For this purpose, the optimal geometrical values for the fillet radius (R_4) and the taper angle (β) of the second region shown in Figure 15 were determined as a result of the DoE - RMS. The variation ranges of the parameters were determined according to the operating volume of the links (Figure 7), model structure and production conditions.

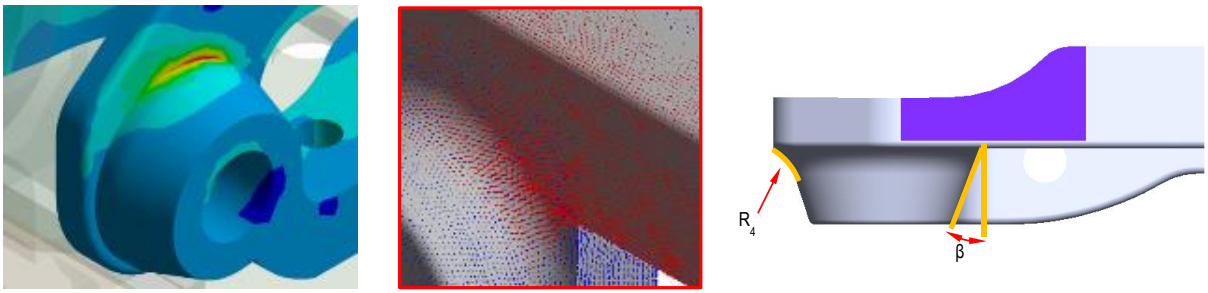

Figure 15. *FEA result of pin slot and selected parameters*

As a result of the analyses performed for the second region, the parameter with the highest effect was determined as the taper angle (β) in the maximum torque model and the fillet radius (R_4) in the lateral force model. In the maximum tensile model, it was observed that the increase in the taper angle increased the stress values. In addition, in the lateral and vertical force model, it was determined that the stress decreases as the fillet radius R_4 increases. Figure 16 shows the response surfaces obtained from these parameters.

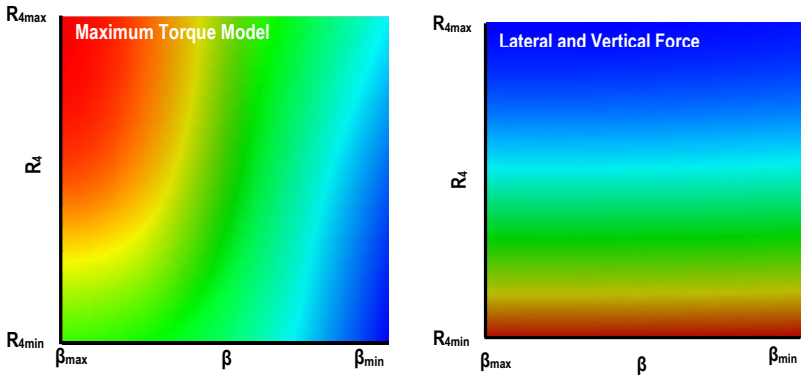

Figure 16. *Response surface plots of the second critical zone parameters*

In order to investigate the stress distribution around the pin slot, the stress values of twelve regions taken at 15° intervals are given in Figure 17 for both force models. As a result of the analyses performed using the optimal values of the parameters, 20% stress reduction was achieved for the first load case and 31% for the second load case.

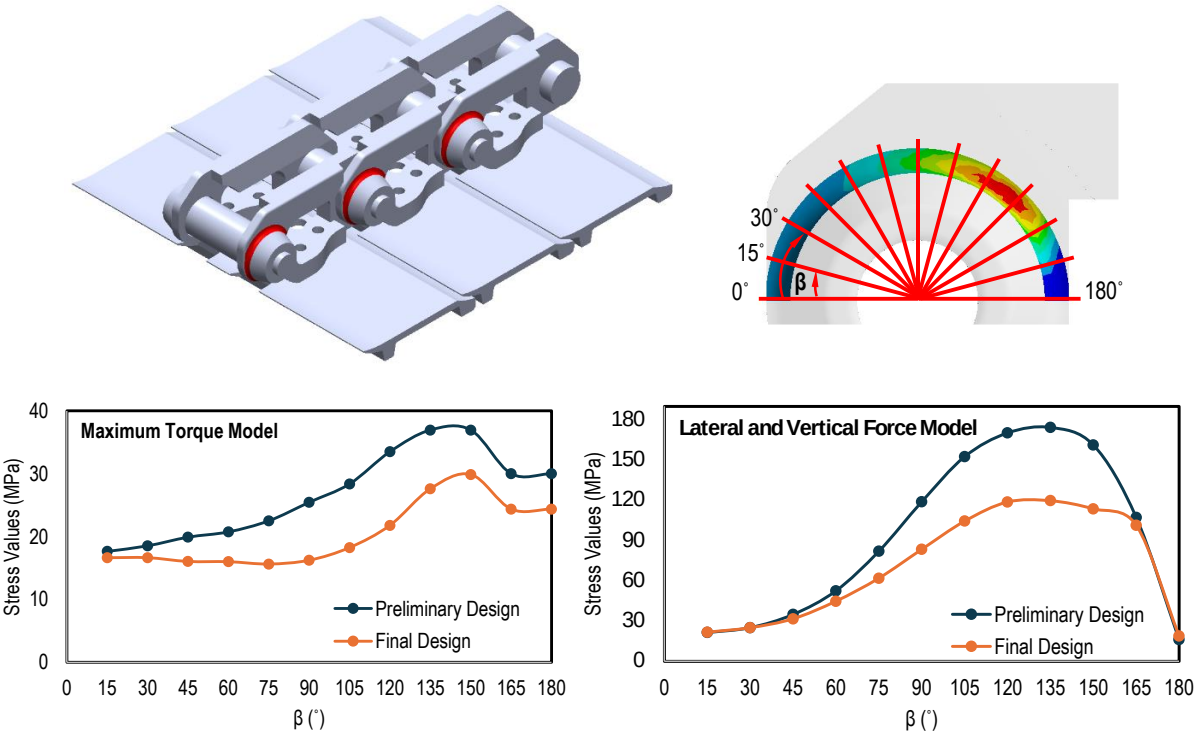

Figure 17. Stress variation at the at the second critical region

The FEA results of the sub-model simulating the operation of the links with each other are shown in Figure 18. In this sub-model, it is seen that the stress concentrations obtained in the critical regions are lower than the failure limits given in the literature as shown in Figure 18.a.

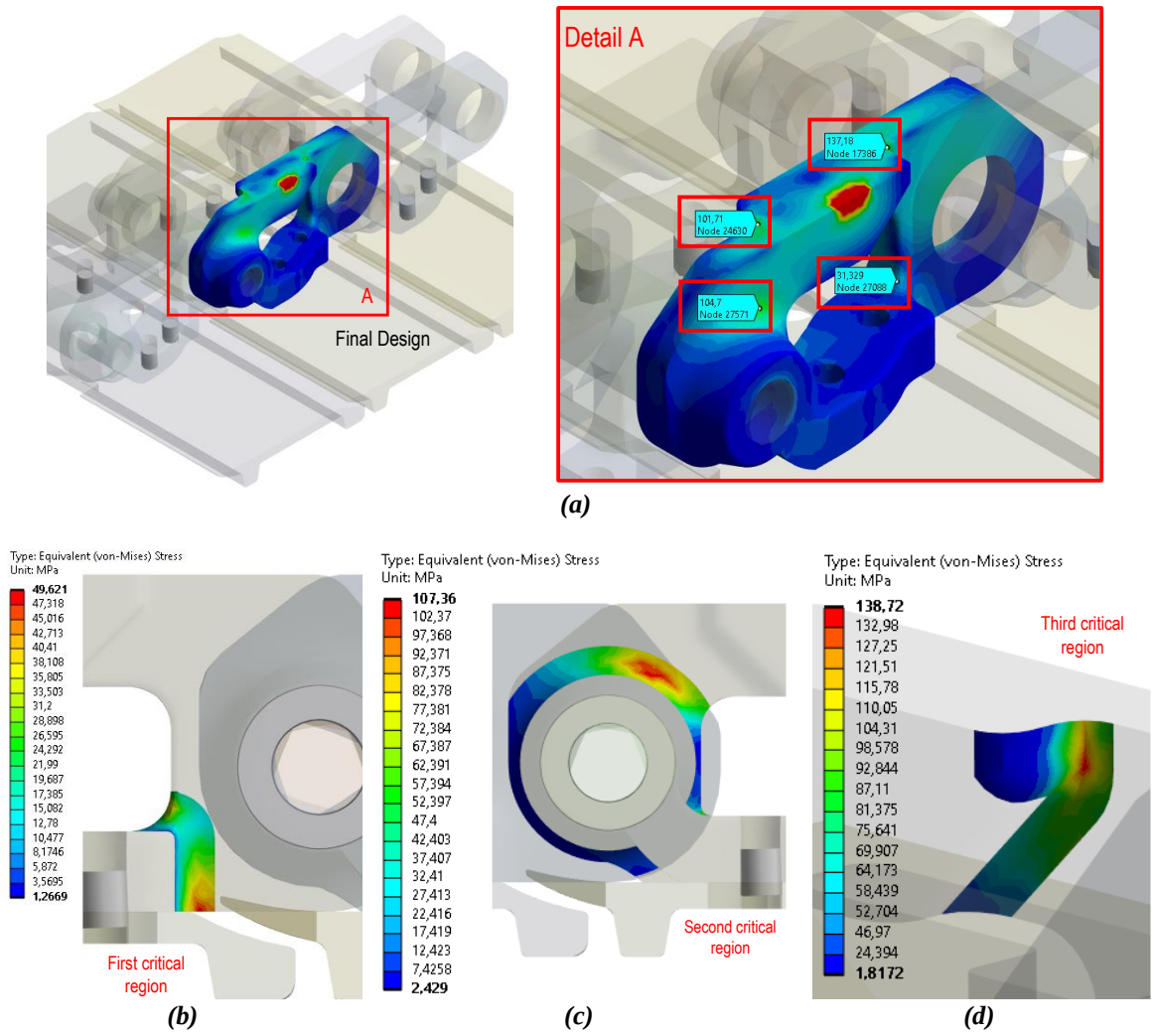

Figure 18. (a) *Sub-model,* ***(b)*** *First critical region,* ***(c)*** *Second critical region and* ***(d)*** *Third critical region*

IV. CONCLUSION

In this study, the design and optimisation processes of the link to be used in the steel track walking system of a tracked vehicle are summarised. Firstly, a preliminary model was created by considering various applied design examples and design constraints determined according to the operating envelope of the link. In this envelope, the penetration of the links in the whole relative rotation angle range is considered. The distances between the drive wheel and the links were also taken into account. Two different Finite Element (FE) models were built: the maximum tension force resulting from the maximum drive torque, and the contact forces caused by the roller contacts in addition to the tension force. With the help of these models, three critical regions in terms of stress concentration were determined on the link. To reduce the stress concentrations in these regions, seven structural design parameters were selected on the component. Using these parameters, a new link design was built using dimensional values obtained from a DoE-based study. The FE analyses for the first case showed that it is possible to reduce the stress concentration approximately 61%, 55% and 20% at the first, second and third critical regions, respectively. For the second load model, the improvement percentages are 63%, 26% and 31% in the same order. An FEA of the sub-model including the new link geometry was also carried out under the same loading conditions. As a result, the stress values at the critical regions of the new link design were found to be below the failure limits reported in the literature.

This paper summarises the design methodology of a track link using simplified ground contact models. It is possible to obtain different designs by using more complex track contact force models.

ACKNOWLEDGEMENTS: The authors are grateful to Smart İş Makinaları San. Tic. A.Ş. and Mr. Sercan Okan for technical support. The technical material presented in this study is published with the permission of Smart İş Makinaları San. Tic. A.Ş. Some technical details of the system are not given in the study due to the confidentiality policy of Smart İş Makinaları San. Tic. A.Ş.

V. REFERENCES

[1] J. Y. Wong and W. Huang, "Wheels vs. tracks – A fundamental evaluation from the traction perspective," *Journal of Terramechanics*, vol. 43, no. 1, pp. 27-42, 2006.

[2] J. Y. Wong, "Dynamics of tracked vehicles," *Vehicle System Dynamics*, vol. 28, no. 2-3, pp. 197-219, 1997.

[3] S. M. Bošnjak, M. A. Arsic, N. D. Zrnic, Z. D. Odanovic, and M. D. Dordevic, "Failure analysis of the stacker crawler chain link," *Procedia Engineering*, vol. 10, pp. 2244-2249, 2011.

[4] Z. W. Yu, X. L. Xu, and X. Mu, "Failure investigation on the cracked crawler pad link," *Engineering Failure Analysis*, vol. 17, no. 5, pp. 1102-1109, 2010.

[5] S. M. Bošnjak, D. B. Momčilović, Z. D. Petković, M. P. Pantelić, and N. B. Gnjatović, "Failure investigation of the bucket wheel excavator crawler chain link," *Engineering Failure Analysis*, vol. 35, pp. 462-469, 2013.

[6] Y. Li, D. He, Q. Si, and X. Meng, "Effect of track shoes structural parameters on traction performance of unmanned underwater tracked bulldozer," *Ocean Engineering*, vol. 237, p. 109655, 2021.

[7] H. Zhao, G. Wang, H. Wang, Q. Bi, and X. Li, "Fatigue life analysis of crawler chain link of excavator," *Engineering Failure Analysis*, vol. 79, pp. 737-748, 2017.

[8] M. A. Arsić, S. M. Bošnjak, Z. D. Odanović, M. M. Dunjić, and A. M. Simonović, "Analysis of the spreader track wheels premature damages," *Engineering Failure Analysis*, vol. 20, pp. 118-136, 2012.

[9] M. M. Topaç, K. Polat, ve O. Çolak, "Çelik paletli yürüyüş sisteminde yapısal emniyetin bakla-makara temas konumuna bağlı değişiminin sayısal incelemesi," INCOHIS 2023: Int. Cong. of New Horizons in Sciences, İstanbul, 2023.

[10] D. Dudek, S. Frydman, W. Huss, and G. Pękalski, "The L35GSM cast steel—Possibilities of structure and properties shaping at the example of crawler links," *Archives of Civil and Mechanical Engineering*, vol. 11, no. 1, pp. 19-32, 2011.

[11] M. G. Bekker, *Theory of Land Locomotion*, Michigan, USA: University of Michigan Press, 1956, pp. 232-282.

[12] J. Y. Wong, *Theory of Ground Vehicles*, 3rd ed., New York, USA: John Wiley & Sons, 2001, pp. 388-431.

[13] T. Amago, “Sizing optimization using response surface method in FOA,” *R&D Review of Toyota CRDL*, vol. 37, no. 1, pp. 1-7, 2002.

[14] M. Aydın and Y. S. Ünlüsoy, “Optimization of suspension parameters to improve impact harshness of road vehicles,” *The International Journal of Advanced Manufacturing Technology*, vol. 60, pp. 743-754, 2012.

[15] D. C. Montgomery, *Design and Analysis of Experiments*, 5th ed., New Jersey, USA : John Wiley & Sons, 2000, pp. 489-569.

[16] R. H. Myers, D. C. Montgomery, and C. M. Anderson-Cook, *Response Surface Methodology, Process and Product Optimization Using Design of Experiments*, 3rd ed., New Jersey, USA: John Wiley & Sons, 2009, pp. 1-349.

[17] B. Gelman and M. Moskvin, *Farm Tractors*, Moscow, : Mir Publishers, 1975, pp. 100-150.

[18] *Komatsu D80A-12, D85A-12 Bulldozers Shop Manual*, Tokyo, Japan : Komatsu, Ltd., pp. 12/05-12/07.